Research Article

MAP4K4 induces early blood-brain barrier damage in a murine subarachnoid hemorrhage model

https://doi.org/10.4103/1673-5374.290904

Received: November 11, 2019

Peer review started: December 3, 2019

Accepted: December 25, 2019

Published online: August 24, 2020

Zheng Zou[1, 2, #], Yu-Shu Dong[2, #], Dong-Dong Liu[2, 3], Gen Li[2, 3], Guang-Zhi Hao[2], Xu Gao[2], Peng-Yu Pan[2, *], Guo-Biao Liang[2, *]

Graphical Abstract *MAP4K4 aggravates tight junction degradation after subarachnoid hemorrhage*

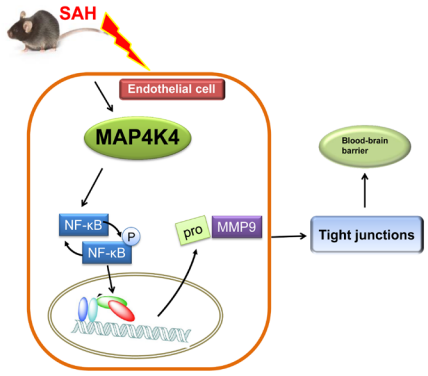

Abstract

Sterile-20-like mitogen-activated protein kinase kinase kinase kinase 4 (MAP4K4) is expressed in endothelial cells and activates inflammatory vascular damage. Endothelial cells are important components of the blood-brain barrier. To investigate whether MAP4K4 plays a role in the pathophysiology of subarachnoid hemorrhage, we evaluated the time-course expression of MAP4K4 after subarachnoid hemorrhage. A subarachnoid hemorrhage model was established using the intravascular perforation method. The model mice were assigned to four groups: MAP4K4 recombinant protein, scramble small interfering RNA, and MAP4K4 small interfering RNA were delivered by intracerebroventricular injection, while PF-06260933, a small-molecule inhibitor of MAP4K4, was administrated orally. Neurological score assessments, brain water assessments, Evans blue extravasation, immunofluorescence, western blot assay, and gelatin zymography were performed to analyze neurological outcomes and mechanisms of vascular damage. MAP4K4 expression was elevated in the cortex at 24 hours after subarachnoid hemorrhage, and colocalized with endothelial markers. MAP4K4 recombinant protein aggravated neurological impairment, brain edema, and blood-brain barrier damage; upregulated the expression of phosphorylated nuclear factor kappa B (p-p65) and matrix metalloproteinase 9 (MMP9); and degraded tight junction proteins (ZO-1 and claudin 5). Injection with MAP4K4 small interfering RNA reversed these effects. Furthermore, administration of the MAP4K4 inhibitor PF-06260933 reduced blood-brain barrier damage in mice, promoted the recovery of neurological function, and reduced p-p65 and MMP9 protein expression. Taken together, the results further illustrate that MAP4K4 causes early blood-brain barrier damage after subarachnoid hemorrhage. The mechanism can be confirmed by inhibiting the MAP4K4/NF-κB/MMP9 pathway. All experimental procedures and protocols were approved by the Experimental Animal Ethics Committee of General Hospital of Northern Theater Command (No. 2018002) on January 15, 2018.

Key Words: brain; central nervous system; injury; pathways; rat; recovery; regeneration; repair

Chinese Library Classification No. R459.9; R363; R364

Introduction

Early brain injury (within 72 hours) was recently revealed to be a main contributor to the poor prognosis of subarachnoid hemorrhage (SAH) patients (Chen et al., 2014b). The pathophysiology of early brain injury after SAH involves injury of the neural vascular network, which contains the arterioles, capillaries, venules, astrocytes, neurons, microglia, surrounding support cells, and extracellular matrix (Zhang et al., 2012). The blood-brain barrier (BBB), which is a unit of the neural vascular network, plays a pivotal role in controlling the exchange of substances between the blood and the brain. Accumulating evidence suggests that targeting the BBB might provide benefits for SAH patients, but the precise mechanisms of BBB damage remain elusive (Xu et al., 2017; Sun et al., 2019).

[1]Department of Neurosurgery, General Hospital of Northern Theater Command (General Hospital of Shenyang Military Command), The Graduate Training Base of Liaoning Medical College, Shenyang, Liaoning Province, China; [2]Department of Neurosurgery, General Hospital of Northern Theater Command (General Hospital of Shenyang Military Command), Shenyang, Liaoning Province, China; [3]Dalian Medical University, Dalian, Liaoning Proivnce, China

*Correspondence to: Peng-Yu Pan, MD, PhD, panpengyu09@sina.com; Guo-Biao Liang, MD, PhD, liangguobiao6708@163.com.

#Both authors contributed equally to this article.

https://orcid.org/0000-0001-8694-5483 (Peng-Yu Pan); https://orcid.org/0000-0001-6332-190X (Guo-Biao Liang)

Funding: *This work was supported by the National Natural Science Foundation of China, Nos. 81971133 (to GBL), 81671313 (to YSD); the Science and Technology Project of Liaoning Province of China, No. 20180550504 (to PYP); the Medical Science Youth Breeding Project of Chinese People's Liberation Army, No. 17QNP053 (to YSD); the China Postdoctoral Science Foundation, No. 2016M592951 (to YSD).*

How to cite this article: *Zou Z, Dong YS, Liu DD, Li G, Hao GZ, Gao X, Pan PY, Liang GB (2021) MAP4K4 induces early blood-brain barrier damage in a murine subarachnoid hemorrhage model. Neural Regen Res 16(2):325-332.*

Numerous findings have demonstrated that inflammatory reactions are the major contributor to BBB damage (Li et al., 2016; Xu et al., 2017; Sun et al., 2019). Matrix metalloproteinase 9 (MMP9) belongs to the matrix metalloproteinase protein family, and is reportedly crucial in the degradation of tight junctions and collagens, which make up the structure of the BBB (Sehba et al., 2012). Endothelial cells, located in the inner surface of vessels, secrete MMP9 under inflammatory conditions (Yang et al., 2014). Some drugs, including sulforaphane, AE1-329, and LP17, have been reported to reduce BBB injury after SAH, but the exact mechanisms remain elusive (Jang and Cho, 2016; Xu et al., 2017; Sun et al., 2019).

The sterile-20-like mitogen-activated protein kinase kinase kinase kinase 4 (MAP4K4) is expressed in endothelial cells and contributes to both atherosclerosis (Roth Flach et al., 2015) and inflammation (Aouadi et al., 2009). Vascular inflammation is considered to be an important process in BBB damage (Chen et al., 2014b), but it remains unknown whether MAP4K4 plays a key role in BBB injury after SAH. We speculated that targeting MAP4K4 after SAH may attenuate early brain injury by decreasing MMP9-associated BBB disruption.

Materials and Methods

Animals

In this study, 402 adult male C57B6J mice weighing 22–30 g and aged 3 months were provided by the Experimental Animal Center of the General Hospital of Northern Theater Command (General Hospital of Shenyang Military Command, Shenyang, China; license No. SCXK (Jing) 2014-0004). Mice were housed in a reversed 12-hour light/dark cycle environment. All experimental procedures and protocols were approved by the Experimental Animal Ethics Committee of the General Hospital of Northern Theater Command (approval No. 2018002) on January 15, 2018. The experimental procedure followed the United States National Institutes of Health Guide for the Care and Use of Laboratory Animals (NIH Publication No. 85-23, revised 1996).

Experimental design

The present study contained four stepwise experiments.

Experiment I

Protein expression differences of MAP4K4 over time and the cellular location of MAP4K4 after SAH were evaluated. For western blot experiments, 42 mice were randomly assigned to seven groups: sham, SAH 3-hour, SAH 6-hour, SAH 12-hour, SAH 24-hour, SAH 48-hour, and SAH 72-hour groups (n = 6 per group; **Table 1**). MAP4K4 expression was detected by western blot assay in the cortex isolated from the ipsilateral (left) hemisphere. Six additional mice were assigned to the sham or SAH 24-hour groups for immunohistochemical experiments (n = 3 per group). Immunostaining of MAP4K4 and lectin (an endotheliocyte marker) was performed at 24 hours after SAH to confirm the expression of MAP4K4 on endothelial cells in the cortex.

Experiment II

To evaluate the intrinsic function of MAP4K4 and screen for the effective dose of MAP4K4 recombinant protein, 159 adult C57B6J mice were randomly assigned to eight groups: sham (n = 25), SAH (n = 12), SAH + normal saline (NS) (2 μL, n = 19), SAH + MAP4K4 10 ng/μL (n = 12), SAH + MAP4K4 50 ng/μL (2 μL, n = 19), SAH + MAP4K4 200 ng/μL (2 μL, n = 12), SAH + scramble (Scr) siRNA (2 μL, n = 25), and SAH + MAP4K4 siRNA (n = 25) groups (**Table 2**). Neurological impairment was evaluated via the modified Garcia score at 24 and 72 hours, as well as by the beam balance test (n = 6). Furthermore, brain water content was evaluated at 24 and 72 hours (n = 6). Evans blue permeability assessment (n = 6) was performed at 24 hours post SAH to evaluate BBB injury.

Experiment III

To investigate possible pathways of BBB damage, 60 adult C57B6J mice were assigned to five groups (n = 12 per group): sham, SAH + NS, SAH + MAP4K4 50 ng/μL, SAH + Scr siRNA, and SAH + MAP4K4 siRNA groups. Western blot assays were performed to detect phosphate-nuclear factor kappa-B (NF-κB; p-p65), zonula occludens-1 (ZO-1) and claudin 5 expression (n = 6; **Table 3**). Zymography was used to detect MMP9 levels in the ipsilateral hemisphere of each group (n = 6). Immunostaining was also performed at 24 hours after SAH induction to detect endothelial continuity in the cortex (n = 3).

Experiment IV

To investigate the effects of PF-06260933 (PF), a MAP4K4 inhibitor, and screen for the optimal dose, 135 adult C57B6J mice were used. Mice were assigned to the sham (n = 31), SAH (n = 12), SAH + vehicle (double-distilled water, n = 31), SAH + PF 1 mg/kg (n = 12), SAH + PF 10 mg/kg (n = 31), and SAH + PF 100 mg/kg (n = 12) groups. The 1, 10, or 100 mg/kg PF (Merck, Darmstadt, Germany) was intragastrically administered at 15 minutes after SAH. Neurological impairment was assessed by the modified Garcia score and beam balance test at 24 and 72 hours after SAH (n = 6; **Table 4**). Brain water content (n = 6) and Evans blue extravasation (n = 6) were used to analyze BBB injury. Tight junction protein degradation was evaluated by immunohistochemistry (n = 3), while western blot assays (n = 6) were performed to detect p-p65, ZO-1, and claudin 5 expression. Gelatin zymography was used to investigate the protein level of MMP9 (n = 6).

SAH models

Endovascular puncture models were established as previously described (Pan et al., 2017). Mice were anesthetized by intraperitoneal injection of pentobarbital sodium (40 mg/kg), and placed in a supine position. The left common carotid artery was isolated and the bifurcation was exposed by blunt

Table 1 | **Intervention information of experiment I**

		SAH					
Experiment I (n=48)	Sham	3 h	6 h	12 h	24 h	48 h	72 h
Western blot	6	6	6	6	6	6	6
Immunofluorescence staining	3				3		

SAH: Subarachnoid hemorrhage.

Table 2 | **Intervention information of experiment II**

Experiment II (n=159)	Sham	SAH	SAH+vehicle	SAH+MAP4K4 10 ng/μL	SAH+MAP4K4 50 ng/μL	SAH+MAP4K4 200 ng/μL	SAH+Scramble (Scr) siRNA	SAH+MAP4K4 siRNA
24 h siRNA effiency	6						6	6
24 h behavior test+brain water content	6	6	6	6	6	6	6	6
72 h behavior test+brain water content	6	6	6	6	6	6	6	6
24 h Evans blue extravasation	6		6		6		6	6
24 h Immunofluorescence staining	3		3		3		3	3

MAP4K4: Mitogen-activated protein kinase kinase kinase kinase 4; SAH: subarachnoid hemorrhage.

dissection. The left external carotid artery was exposed distally to the digastric muscle, and the left internal carotid artery was exposed distally to the origin of the pterygopalatine artery. The external carotid artery was sheared distally, being careful to leave the longest possible stump. A 5-0 nylon suture was inserted from the left external carotid artery stump into the internal carotid artery, then pushed 3 mm through the bifurcation of the left internal carotid artery until resistance was felt (model establishment success). Internal carotid artery patency was confirmed after the suture was withdrawn, and the stump of the external carotid artery was then ligated. In the sham group, the operation was identical, but the suture was not pushed through the bifurcation of the internal carotid artery.

Intracerebroventricular injection

Intracerebroventricular injections were conducted as previously described (Zhao et al., 2017). A 1-mm-diameter hole was drilled 1 mm lateral to the bregma on the skull, without perforating the dura (Paxinos et al., 2001). The needle of a 10-μL Hamilton syringe (Microliter 701; Hamilton Company, Reno, NV, USA) was stereotactically inserted vertically into the hole to a depth of 3.0 mm, under the horizontal plane of the bregma. The needle penetrated the dura and was inserted into the left lateral ventricle. A 2 μL volume of recombinant MAP4K4 protein (Abnova, Taiwan, China) solution was infused at a rate of 0.2 μL/min at 1 hour after SAH induction, while 2 μL of MAP4K4 siRNA (Santa Cruz Biotechnology, Santa Cruz, CA, USA; 500 pmol in a 2-μL mixture of 1:1 RNase-free water and lipofectamine) or Scr siRNA (Santa Cruz Biotechnology; 500 pmol in a 2-μL mixture of 1:1 RNase-free water and lipofectamine) was infused at an identical rate at 48 hours before SAH induction.

SAH grade

The severity of SAH mice was evaluated with an 18-point grading system, as previously described (Chen et al., 2015). The basal cistern was divided into six areas, and each area was scored from 0–3 depending on the amount of clot in the SAH. The total score (0–18 points) was a summation of the six areas. Mice were excluded when scores < 8.

Neurological outcome evaluation

Neurological deficits were assessed as previously described (Dong et al., 2016). The modified Garcia score (Chen et al., 2015) and beam balance test (Wu et al., 2010) were used at 24 or 72 hours after SAH. The Garcia score included (1) spontaneous activity, (2) symmetry in the movement of all four limbs, (3) symmetry of the forelimbs, (4) climbing, (5) response to touch on either side of the trunk, and (6) response to vibrissae touch. Each part was scored from 0–3, as follows: 0, complete deficit; 1, deficit with function; 2, mild deficit; and 3, normal. The means of the neurological scores were from two blinded observers.

The procedures of the beam balance test were as follows: a beam (length 90 cm, width 1 cm) was placed between two platforms. Mice were pre-adapted to run freely on the beam before the test. Next, mice were placed onto the middle of the beam and ran to either side of the platform. Mice were scored based on their running performance, as follows: 0, fell off the beam within 40 seconds without moving; 1, did not move but stayed on the beam for at least 40 seconds; 2, moved not more than half the distance to the platform in 40 seconds and stayed on the beam for at least 25 seconds; 3, moved more than half the distance to the platform in 40 seconds and stayed on the beam for at least 25 seconds; 4, moved onto either platform within 40 seconds or moved to the platform within 25 seconds but did not get onto the platform; and 5, moved onto either platform in 25 seconds. An average score was calculated from three trials.

Brain water content

The brain specimens were carefully removed from the skull and separated into the left and right cerebral hemispheres, cerebellum, and brain stem, and then weighed (wet weight) on an analytical balance as previously described (Pan et al., 2020). The brains were then dried at 55°C in a drying system (DHG-9240A, Jing Hong Laboratory Instrument, Shanghai, China) for 48 hours, and then weighed again (dry weight). The final brain water content was calculated according to the formula:

$$\text{Brain water content (\%)} = \frac{\text{Wet weight} - \text{Dry weight}}{\text{Wet weight}} \times 100$$

Measurement of Evans blue extravasation

Evans blue extravasation was measured as previously described (Pan et al., 2017). After anesthesia with pentobarbital sodium (40 mg/kg) via intraperitoneal injection at 24 hours post SAH, Evans blue dye (2%, 5 mL/kg; Sigma-Aldrich, St. Louis, MO, USA) was injected into the left femoral vein over 2 minutes and allowed to circulate for 60 minutes. Phosphate-buffered saline (PBS) was then perfused through the left ventricle until clear liquid flowed from the incision of the right auricle. The brain samples were removed, and the left cerebral hemispheres were rapidly isolated and weighed. After being homogenized in saline, the samples were centrifuged at 15,000 × *g* for 30 minutes. The resulting supernatant was collected and mixed with the same volume of trichloroacetic acid. The mixture was incubated for at least 10 hours at 4°C, and then centrifuged again at 15,000 × *g* for 30 minutes. Next, the supernatant was collected and Evans blue dye was detected spectrophotometrically using a microplate reader (Thermo Fisher Scientific, Shanghai, China) at 610 nm (ultraviolet wavelength).

Table 3 | **Intervention information of experiment III**

Experiment III (*n*=60)	Sham	SAH+ vehicle	SAH+MAP4K4 50 ng/μL	SAH+Scramble (Scr) siRNA	SAH+MAP4K4 siRNA
24 h Western blot assay	6	6	6	6	6
24 h Zymography	6	6	6	6	6

MAP4K4: Mitogen-activated protein kinase kinase kinase kinase 4; SAH: subarachnoid hemorrhage.

Table 4 | **Intervention information of experiment IV**

Experiment IV (*n*=135)	Sham	SAH	SAH+vehicle	SAH+PF 1 mg/kg	SAH+PF 10 mg/kg	SAH+PF 100 mg/kg
24 h behavior text+brain water content	6	6	6	6	6	6
72 h behavior test+brain water content	6	6	6	6	6	6
24 h Evans blue extravasation	6		6		6	
24 h Immunofluorescence staining	3		3		3	
24 h Western blot assay	6		6		6	
24 h Zymography	6		6		6	

MAP4K4: Mitogen-activated protein kinase kinase kinase kinase 4; PF: PF-06260933; SAH: subarachnoid hemorrhage.

Immunofluorescence staining

Immunofluorescence staining was performed as previously described (Hao et al., 2016). Mice were deeply anesthetized by intraperitoneal injection of pentobarbital (40 mg/kg), perfused with pre-cooled PBS to remove blood, and fixed with 4% paraformaldehyde at 24 hours post SAH. Brain samples were immersed in 4% paraformaldehyde for 24 hours and then soaked in 40% sucrose for 24 hours. Coronal brain sections (10 μm) at 1.5 mm posterior to bregma were microtomed using a cryostat (Leica, Eisfeld, Germany) and immersed in 0.3% Triton X-100 for 1 hour at room temperature. Slides were then blocked with 5% donkey serum for 1 hour at room temperature before being incubated with anti-claudin 5 (tight junction protein marker, rabbit polyclonal; Abcam, Cambridge, UK), anti-MAP4K4 (rabbit polyclonal; Proteintech Group, Rosemont, IL, USA), and lectin (endotheliocyte marker; Vector Laboratories, Burlingame, CA, USA) antibodies at 4°C overnight. Sections were then incubated with appropriate secondary antibodies (donkey and goat polyclonal, 1:200; Cat#: A-11008, A-31572; Thermo Fisher Scientific) for 4 hours at room temperature. The sections were washed with PBS, and 4′,6-diamidino-2-phenylindole (DAPI; Beyotime, Shanghai, China) was added and incubated for 10 minutes at room temperature. After washing with PBS, the basal cortex was imaged using a fluorescence microscope (Olympus, Melville, NY, USA).

Western blot assay

Western blot assays were performed as previously described (Feng et al., 2017). Briefly, cytoplasmic, nuclear, and membrane proteins (cytoplasmic protein for detecting MAP4K4, nuclear protein for detecting p-p65, and membrane protein for detecting claudin 5 and ZO-1) were extracted from the ipsilateral hemisphere before being separated stepwise using a Subcellular Protein Fractionation Kit for Tissues (Pierce Biotechnology, Rockford, IL, USA) according to the manufacturer's guidelines. Equal amounts of total protein (30 μg) were loaded into each lane of 10% sodium dodecyl sulfate polyacrylamide gel electrophoresis gels. The proteins were separated by electrophoresis and then transferred onto a polyvinylidene fluoride membrane. The membrane was subsequently blocked with blocking buffer for 2 hours at room temperature, and then incubated overnight at 4°C with the following antibodies: anti-claudin 5, anti-ZO-1, anti-phosphate-p65 (1:500, Cat# ab15106, ab96587, ab86299; Abcam) and anti-MAP4K4 (Cat# 55247-1-AP, Proteintech Group). β-Actin and histone H3 were used as the internal loading controls (1:2000; Cat# sc-47778, Santa Cruz Biotechnology; 1:500, Cat# PA5-16183, Thermo Fisher Scientific). The membranes were then incubated with the corresponding secondary antibodies (goat, 1:200, Cat# G-21234, G-21040; Thermo Fisher Scientific) for 2 hours at room temperature. The blots were imaged using enhanced Chemilucent Plus (Merck). Data were analyzed by densitometry using Quantity One (Bio-Rad, Berkeley, CA, USA). The densities of all bands were expressed as ratios against the sham group.

Gelatin zymography

Gelatin zymography was performed as previously described (Pan et al., 2017). Protein was extracted from the ipsilateral hemisphere of the mouse brain and separated by electrophoresis on 8% tris-glycine gel containing 0.1% gelatin, in tris-glycine sodium dodecyl sulfate running buffer. After electrophoresis, MMP9 was renatured by incubating the gel in renaturing buffer (Thermo Fisher Scientific) for 30 minutes at room temperature. The gel was then incubated in developing buffer (Thermo Fisher Scientific) before divalent metal cations were added and incubated at 37°C overnight. The gel was then washed with PBS and immersed in SimplyBlue (Thermo Fisher Scientific) for 30 minutes, with gentle agitation, to develop the MMP9 bands. The gel was imaged with a scanner and quantified using ImageJ software v1.48 (National Institute of Mental Health, Bethesda, MD, USA).

Statistical analysis

All data are expressed as the mean ± SD, and were analyzed using SPSS 18.0 software (SPSS, Chicago, IL, USA). Differences between groups were tested using one-way analysis of variance and Tukey's *post-hoc* test. $P < 0.05$ was considered statistically significant.

Results

Mortality (Experiments I–IV)

In Experiment I, (0/6) mice died in the sham group, (1/6) died in the SAH 3-hour group, (1/6) died in the SAH 6-hour group, (0/6) died in the SAH 12-hour group, and (1/6) died in the SAH 48-hour group, caused by severe hemorrhagic volume. At 24 hours post SAH, mortality among the groups was as follows: (3/18) in the SAH group, (5/52) in the SAH + vehicle group, (1/6) in the SAH + MAP4K4 10 ng/μL group, (3/27) in the SAH + MAP4K4 50 ng/μL group, (1/6) in the SAH + MAP4K4 200 ng/μL group, (2/33) in the SAH + Scr siRNA group, and (2/33) in the SAH + MAP4K4 siRNA group. At 72 hours post SAH, mortality among the groups was as follows: (7/18) in the SAH group, (5/12) in the SAH + vehicle group, (3/6) in the SAH + MAP4K4 10 ng/μL group, (2/6) in the SAH + MAP4K4 50 ng/μL group, (3/6) in the SAH + MAP4K4 200 ng/μL group, (2/6) in the SAH + Scr siRNA group, and (3/6) in the SAH + MAP4K4 siRNA group. In the analysis of the results, 402 mice were involved; the excluded and dead animals were replaced by new ones.

Time course of intrinsic MAP4K4 expression after SAH (Experiment I)

There was a significant increase in MAP4K4 in the ipsilateral hemisphere at 12, 24, 48, and 72 hours after SAH (**Figure 1A** and **B**). Furthermore, immunohistochemical staining in the sham group revealed that MAP4K4 colocalized with lectin, an endothelial marker, in the ipsilateral cortex (**Figure 1C**). At 24 hours post SAH, MAP4K4 was markedly elevated in endothelial cells (**Figure 1C**).

Neurological function after recombinant MAP4K4 delivery and interference of MAP4K4 expression after SAH (Experiment II)

There were no significant differences in SAH grading scores among the groups at 24 and 72 hours ($P < 0.05$; **Figure 2A**). MAP4K4 siRNA effectively inhibited MAP4K4 expression after SAH ($P < 0.05$; **Figure 2B** and **C**). Mice in the SAH group showed significant neurological dysfunction in the modified Garcia test and beam balance test compared with the sham group at 24 hours ($P < 0.05$; **Figure 2D** and **E**). In addition, mice in the SAH + MAP4K4 50 ng/μL and SAH + MAP4K4 200 ng/μL groups had more severe neurological deficits at 24 hours post SAH compared with the SAH + NS group ($P < 0.05$; **Figure 2D** and **E**). Moreover, MAP4K4 siRNA treatment led to improvements in neurological function compared with the SAH + Scr siRNA group at 24 hours ($P < 0.05$; **Figure 2D** and **E**).

BBB leakage after recombinant MAP4K4 delivery and interference of MAP4K4 expression (Experiment II)

Brain edema is considered an independent factor of poor prognosis after SAH, and BBB injury is an essential pathophysiological process that promotes edema (Macdonald and Schweizer, 2017). Mice in the SAH and SAH + NS groups had marked brain edema in the ipsilateral cortex. Brain edema was significantly increased in the SAH + MAP4K4 50 ng/μL and SAH + MAP4K4 200 ng/μL groups compared with the SAH + NS group, while MAP4K4 siRNA pretreatment reversed this effect ($P < 0.05$; **Figure 2F** and **G**). We therefore chose MAP4K4 50 ng/μL for subsequent experiments. Evans blue extravasation in the left hemisphere was increased in the SAH, SAH + NS,

and SAH + Scr siRNA groups at 24 hours after SAH compared with the sham group ($P < 0.05$; **Figure 2H**). Furthermore, MAP4K4 50 ng/μL and 200 ng/μL treatment aggravated Evans blue extravasation compared with the SAH + NS group, while MAP4K4 siRNA infusion significantly reduced Evans blue leakage at 24 hours post SAH ($P < 0.05$; **Figure 2H**).

Tight junction proteins and MMP9 expression after recombinant MAP4K4 delivery and specific inhibition of MAP4K4 expression (Experiment III)

As transmembrane proteins on the BBB, claudins are anchored into protein complexes, such as ZO-1, to maintain BBB integrity. Immunofluorescent staining was performed in the ipsilateral cortex, and the normally continuous structures of endothelial cells (lectin) and claudin 5 were discontinuous at 24 hours post SAH. MAP4K4 recombinant protein treatment worsened these injuries; however, MAP4K4 siRNA infusion reversed these disruptions at 24 hours after SAH (**Figure 3**). These phenomena were speculated to activate NF-κB (p65) and MMP9 signaling. Western blot assay results indicated that the nuclear protein levels of p-p65 in the SAH group were elevated at 24 hours (**Figure 4A** and **B**) after SAH. In addition, MMP9 zymography revealed enhanced MMP9 expression at 24 hours post SAH ($P < 0.05$; **Figure 4E** and **F**). MAP4K4 administration increased the levels of nuclear p-p65 and MMP9 ($P < 0.05$; **Figure 4A**, **B**, **E**, and **F**), and this trend was reversed by MAP4K4 siRNA pretreatment ($P < 0.05$; **Figure 4A**, **B**, **E**, and **F**). The levels of ZO-1 and claudin 5 were decreased after MAP4K4 recombinant protein infusion, but were increased by MAP4K4 siRNA pretreatment ($P < 0.05$; **Figure 4A**, **C**, and **D**).

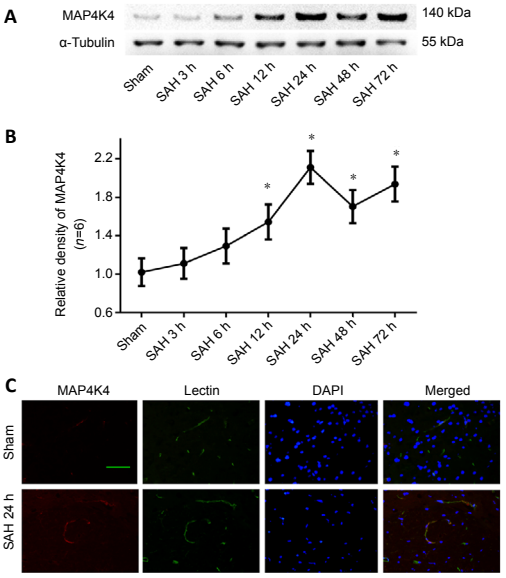

Figure 1 | Time course of intrinsic MAP4K4 expression after SAH (Experiment I).

(A) Representative western blot bands of MAP4K4 expression after SAH. (B) Quantitative analysis of MAP4K4 from the ipsilateral hemisphere; the relative density of each protein was normalized to the sham group. Data are expressed as the mean ± SD ($n = 6$; one-way analysis of variance and Tukey's *post hoc* test). *$P < 0.05$, *vs.* sham group. (C) Representative immunohistochemistry of MAP4K4 (red) and lectin (green) in the sham and SAH group at 24 hours after SAH ($n = 3$). Scale bar: 20 μm. DAPI: 4′,6-Diamidino-2-phenylindole; MAP4K4: sterile-20-like mitogen-activated protein kinase kinase kinase kinase 4; SAH: subarachnoid hemorrhage.

Pharmacological MAP4K4 inhibition and BBB damage post SAH (Experiment IV)

PF, a highly selective small-molecule inhibitor of MAP4K4 (Ammirati et al., 2015), was administered after SAH. SAH grade did not significantly differ among the groups ($P < 0.05$; **Figure 5A**). Doses of 10 and 100 mg/kg PF markedly improved neurological function and reduced brain water content, while 1 mg/kg did not ($P < 0.05$; **Figure 5B**–**E**). There were no significant differences in neurological score and brain water content between the 10 and 100 mg/kg groups, so we chose 10 mg/kg for further experiments ($P < 0.05$; **Figure 5B**–**E**). Evans blue extravasation was reduced by 10 mg/kg PF ($P < 0.05$; **Figure 5F**). Immunohistochemical staining, western blot assay, and zymography results revealed that p-p65 activation and MMP9 expression decreased after PF administration ($P < 0.05$; **Figures 6** and **7**). PF also prevented the decreased protein levels of ZO-1 and claudin 5 ($P < 0.05$; **Figure 7A**, **C**, and **D**).

Discussion

The present study demonstrated that MAP4K4 increased after SAH, remained increased at 24, 48, and 72 hours, and was elevated in endothelial cells. Exogenous MAP4K4 protein administration worsened neurological deficits and brain edema at concentrations of 50 ng/μL and 200 ng/μL, while MAP4K4 silencing effectively reversed these trends.

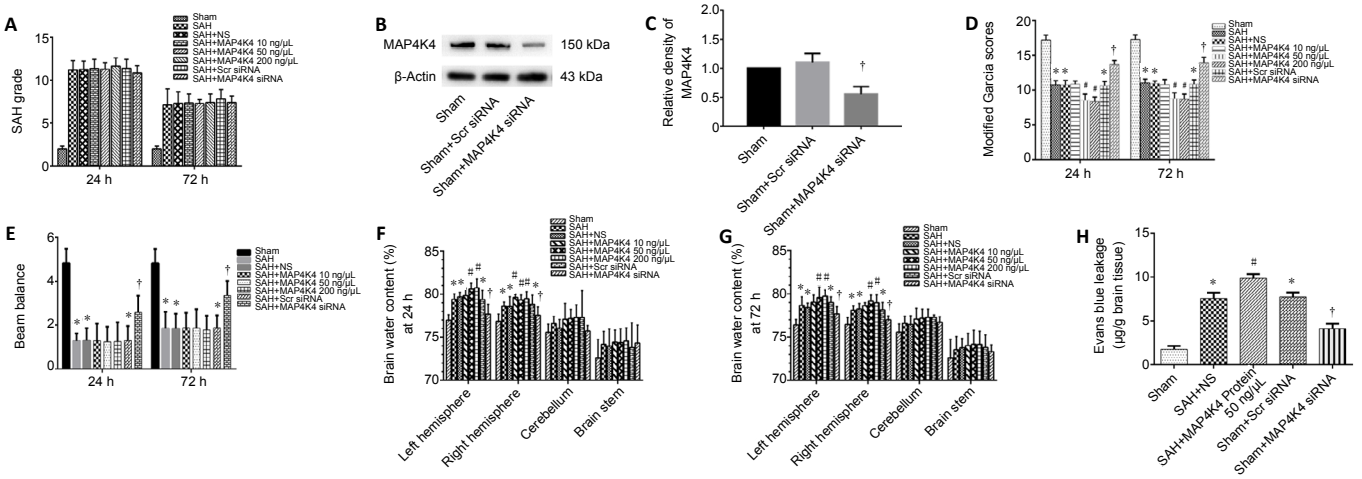

Figure 2 | Neurological functions, brain water content, and blood-brain barrier permeability after recombinant MAP4K4 delivery and MAP4K4 silencing post SAH (Experiment II).

(A) SAH grading scores. (B, C) Representative western blot bands of MAP4K4 siRNA knockdown efficiency at 24 hours post SAH. (D, E) Modified Garcia scores and beam balance test results at 24 and 72 hours. (F, G) Brain water content at 24 and 72 hours after SAH. (H) Evans blue leakage in the ipsilateral hemisphere 24 hours post SAH. Data are expressed as the mean ± SD ($n = 6$; one-way analysis of variance and Tukey's *post hoc* test). *$P < 0.05$, *vs.* sham group; #$P < 0.05$, *vs.* SAH + NS group; †$P < 0.05$, *vs.* SAH + Scr siRNA group. MAP4K4: Sterile-20-like mitogen-activated protein kinase kinase kinase kinase 4; SAH: subarachnoid hemorrhage; Scr: scramble.

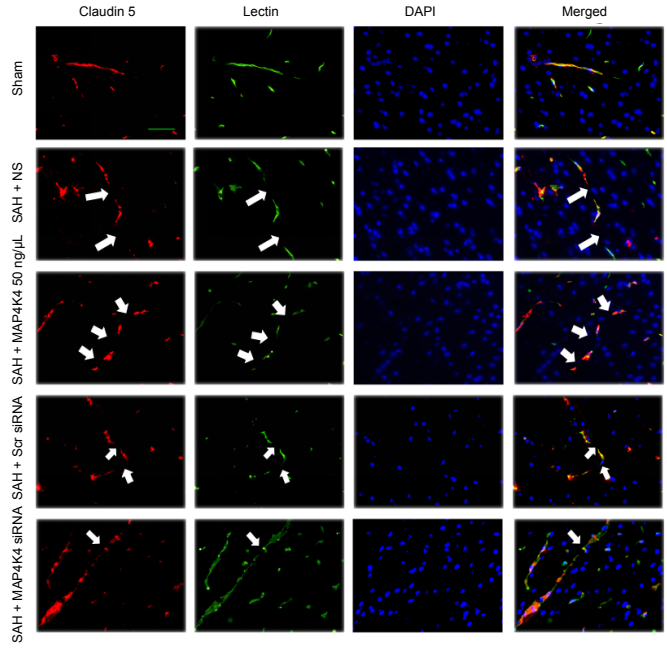

Figure 3 | Continuous endothelial cell and tight junction protein disruption after recombinant MAP4K4 delivery and MAP4K4 silencing post SAH (Experiment III).

Endothelium and tight junction discontinuity was demonstrated by lectin and claudin 5 staining in the ipsilateral cortex after MAP4K4 recombinant protein infusion and MAP4K4 siRNA pretreatment, at 24 hours post SAH, under a fluorescence microscope. *n* = 3. Scale bar: 20 μm. Endothelium and tight junction discontinuity was greater in the SAH group than in the sham group. MAP4K4 increased endothelium and tight junction discontinuity while MAP4K4 siRNA reversed those trends. Arrows indicate discontinuity of endothelial cells and claudin 5. Red: claudin 5; green: lectin; blue: DAPI. DAPI: 4′,6-diamidino-2-phenylindole; MAP4K4: sterile-20-like mitogen-activated protein kinase kinase kinase kinase 4; SAH: subarachnoid hemorrhage; Scr: scramble.

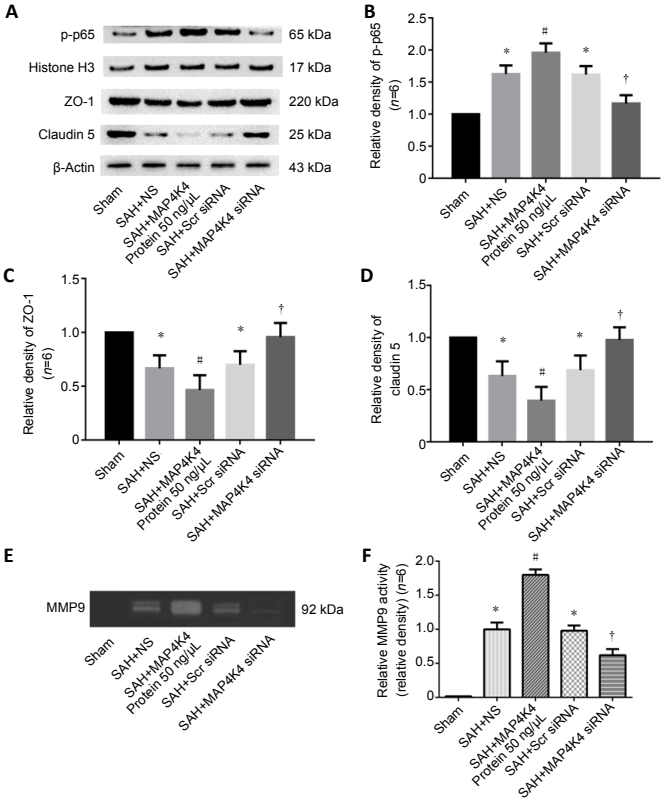

Figure 4 | Protein expression of nuclear p-p65, tight junction proteins, and MMP9 activity in the ipsilateral hemisphere after recombinant MAP4K4 delivery and MAP4K4 silencing post SAH (Experiment III).

(A–D) Protein levels of p-p65, ZO-1, and claudin 5. p-p65 expression levels were elevated at 24 hours, and this effect was enhanced by MAP4K4 infusion and reversed by pretreatment with MAP4K4 siRNA. ZO-1 and claudin 5 expression had the opposite trend. (E, F) Representative gelatin zymography of MMP9 expression revealed that proteinase activity rose at 24 hours after SAH, and was enhanced by MAP4K4 infusion and reversed by pretreatment with MAP4K4 siRNA. The quantified density was normalized to the sham group. Data are expressed as the mean ± SD (*n* = 6; one-way analysis of variance and Tukey's *post hoc* test).*$P < 0.05$, *vs.* sham group; #$P < 0.05$, *vs.* SAH + NS group; †$P < 0.05$, *vs.* SAH + Scr siRNA group. MAP4K4: Sterile-20-like mitogen-activated protein kinase kinase kinase kinase 4; MMP9: matrix metalloproteinase 9; SAH: subarachnoid hemorrhage; Scr: scramble.

Moreover, administration of MAP4K4 induced BBB disruption by interrupting continuous endothelial cells and tight junctions. An investigation of the mechanisms indicated that MAP4K4 enhanced p-p65 nuclear translocation and activated downstream MMP9, which is a main factor in tight junction protein degradation. Taken together, MAP4K4 may be a potential target for reducing BBB degradation after SAH.

MAP4K4, also known as hepatocyte progenitor kinase-like/germinal center kinase-like kinase and Nck-interacting kinase, belongs to the sterile 20 family of kinases. These are expressed broadly in the brain and are involved in many pathophysiological processes, including development (Xue et al., 2001), cell motility (Vitorino et al., 2015), and inflammation (Roth Flach et al., 2015; Tu et al., 2018). MAP4K4 was found to phosphorylate moesin, and then displaces talin from INTb1 to inactivate b1-integrin and cause membrane retraction (Vitorino et al., 2015). MP4K4 is reportedly critical for NF-κB activation and enhances atherosclerosis (Roth Flach et al., 2015). As an atypical MAPK, previous studies have demonstrated that MAP4K4 is upstream of c-Jun NH2-terminal kinase signaling (Su et al., 1997; Collins et al., 2006), while other studies have revealed that MAP4K4 may not be required for MAPK activation (Danai et al., 2013; Wang et al., 2013).

Previous reports have also suggested that endothelial MAP4K4 enhances the upregulation of leukocyte adhesion molecule, promotes monocyte infiltration, and increases chemokine expression (Pannekoek et al., 2013; Vitorino et al., 2015). Atherosclerosis is a chronic disease whose etiological factor is speculated to be vessel inflammation. In the present study, MAP4K4 expression was elevated early (at 12 hours) and induced rapid BBB disruption at 24 hours post SAH, with discontinuous endothelial cells and tight junctions observed. It is difficult to attribute these phenomena to alterations of chemokines and adhesion molecules only. The best explanation may be that MAP4K4 activated NF-κB and downstream MMP9, but further studies are needed before any conclusions can be reached. This is the first report of MAP4K4 involvement in rapid vascular inflammation. In terms of mortality, there were no differences among the groups at 24 or 72 hours. These results are similar to those of our previous publications (Chen et al., 2015; He et al., 2015; Pan et al., 2017; Zhu et al., 2018), and suggest that intracerebral regulation of MAP4K4 preserves neurological function but does not reduce mortality after SAH. This phenomenon may be influenced by complex complications of the circulation system, respiratory system, electrolyte balance, systemic inflammatory response, or severe amounts of clot at the SAH ictus (Chen et al., 2014a; Lantigua et al., 2015).

The BBB is a highly selective neurovascular unit that can prevent harmful substances from entering the brain while allowing nutrients to enter (Keaney and Campbell, 2015). After SAH or other acute neurological injuries, BBB permeability is elevated. This increased permeability leads to blood metabolites directly contacting neurons and surrounding cells, which can cause neuronal death and vasogenic brain edema. Increased BBB permeability at the acute stage of subarachnoid hemorrhage has been reported to correlate

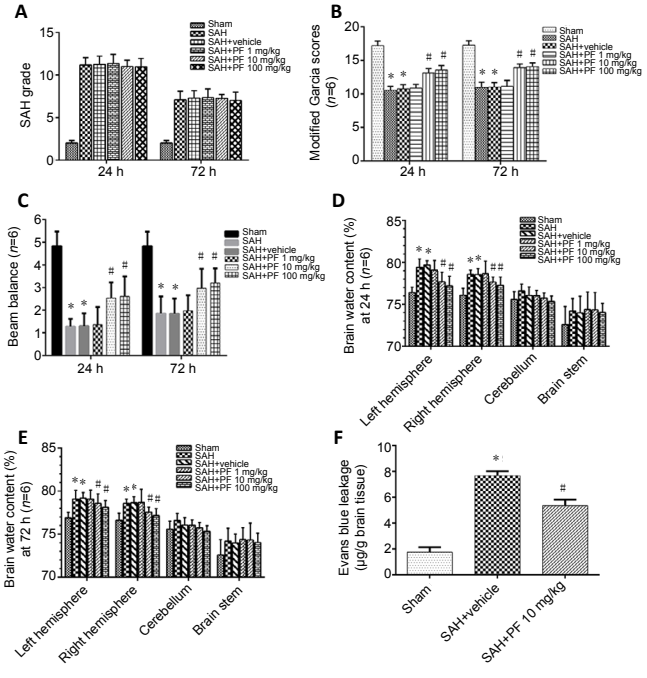

Figure 5 | Neurological function, brain water content, and blood-brain barrier leakage after PF delivery post SAH (Experiment IV).
(A, B) SAH grading scores. (B, C) Modified Garcia scores and beam balance test results. (D, E) Brain water content at 24 and 72 hours after SAH. (F) Evans blue leakage at 24 hours. Data are expressed as the mean ± SD (n = 6; one-way analysis of variance and Tukey's *post hoc* test).*P < 0.05, *vs.* sham group; #P < 0.05, *vs.* SAH + vehicle group. MAP4K4: Sterile-20-like mitogen-activated protein kinase kinase kinase kinase 4; PF: PF-06260933; SAH: subarachnoid hemorrhage.

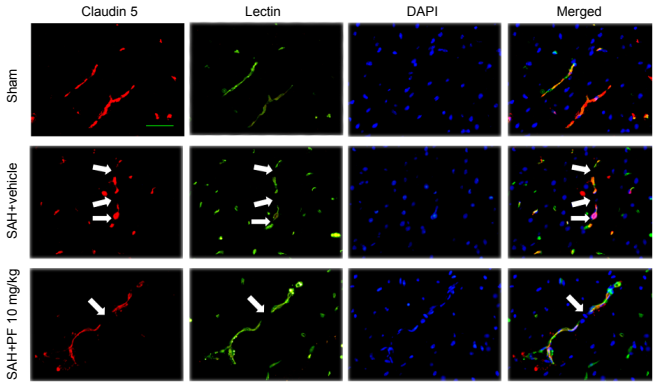

Figure 6 | Continuous endothelial cell and tight junction protein disruption after PF delivery post SAH (Experiment IV).
Endothelium (lectin) discontinuity and tight junction (claudin 5) degradation in the ipsilateral cortex after SAH. Endothelium and tight junction discontinuity was greater in the SAH + vehicle group than in the sham group. Endothelium and tight junction discontinuity was preserved by PF administration. Scale bar: 20 μm. Arrows indicate discontinuity of endothelial cells and claudin 5. Red: claudin 5; green: lectin, blue: DAPI. DAPI: 4′,6-Diamidino-2-phenylindole; PF: PF-06260933; SAH: subarachnoid hemorrhage.

with poorer outcomes in clinical research (Ivanidze et al., 2018; Lublinsky et al., 2019), and is an important manifestation of early brain injury. Endothelial cells are a main component of the BBB; transcellular transport and tight junctions help maintain BBB structure and function (Zhao et al., 2015). Matrix metalloproteinases, and especially MMP9, are essential for the development of vasogenic edema and BBB damage after various brain injuries, including SAH, ischemic stroke, and traumatic brain injury (Feiler et al., 2011; Egashira et al., 2015; Michinaga et al., 2018; Zuo et al., 2019). In the current investigation, we demonstrated that brain edema worsened and Evans blue extravasation increased after SAH, and that

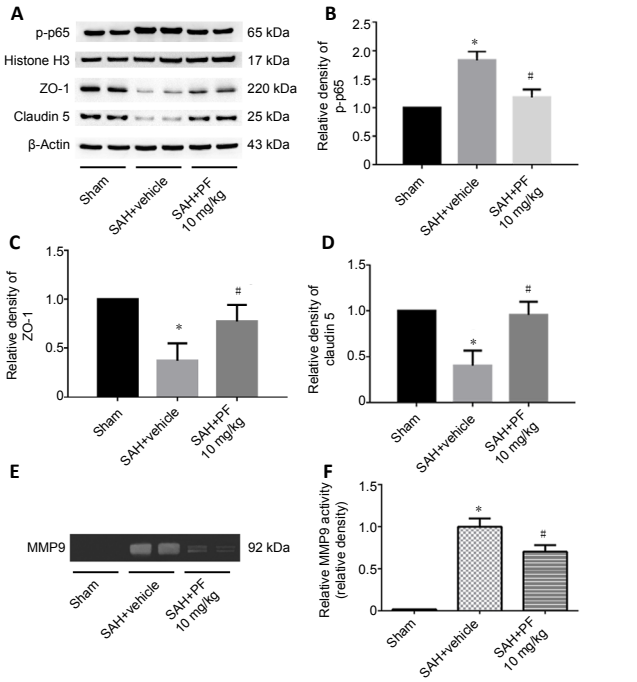

Figure 7 | Protein expression of nuclear p-p65 and tight junction proteins and MMP9 activity in the ipsilateral hemisphere after PF delivery post SAH (Experiment IV).
(A–D) Levels of p-p65 decreased, while the expression of ZO-1 and claudin 5 was restored after PF administration. (E, F) Representative gelatin zymography of MMP9 expression revealed that PF attenuated MMP9 expression after SAH. Data are expressed as the mean ± SD (n = 6; one-way analysis of variance and Tukey's *post-hoc* test).*P < 0.05, *vs.* sham group; #P < 0.05, *vs.* SAH + NS group. MMP9: Matrix metalloproteinase 9; PF: PF-06260933; SAH: subarachnoid hemorrhage.

MAP4K4 expression levels increased in endothelial cells. Moreover, knockdown of MAP4K4 ameliorated downstream NF-κB activation and MMP9 maturation, leading to BBB protection. PF, which is an inhibitor of MAP4K4, has been demonstrated to reduce MAP4K4-induced inflammation (Roth Flach et al., 2015). We also revealed that MAP4K4-induced inflammation was eliminated by PF, and that neurological outcome and BBB disruption were improved by PF treatment after SAH. Together, these results indicate that PF may be a candidate treatment for SAH; however, further clinical trials are needed.

This study had some limitations. Our data are only focused on MAP4K4 expression, while details of the NF-κB/MMP9 pathway were not studied. After SAH, NF-κB translocates to the nucleus, elevates MMP9 transcription, and induces the degradation of basement membrane and tight junction proteins; these effects have been well illustrated in previous studies. In addition, MAP4K4 may be located extracellularly and might affect surrounding cells as a ligand. Consistent with previous studies, we found that endothelial cells expressed high levels of MAP4K4; however, it remains unclear whether the MAP4K4/NF-κB pathway is activated in other cells after SAH. Furthermore, other as-yet-unknown mechanisms of MAP4K4 on MMP9 expression cannot be excluded. In future studies, more data are needed regarding the expression of MAP4K4 in other cell types and to elucidate the precise mechanisms of downstream NF-κB and MMP9.

In summary, MAP4K4 plays a vital role in early brain injury after SAH. Increasing MAP4K4 leads to rapid vascular inflammation and BBB disruption, caused by the NF-κB/MMP9 pathway. Genetic and pharmacological inhibition of MAP4K4 protects neurological function and BBB integrity. By targeting MAP4K4, new light may be shed on the management of SAH patients.

Author contributions: *Study design: YSD, XG, and PYP; experiment performance: ZZ, GBL, DDL, and GZH; data analysis: ZZ; manuscript preparation and revision: PYP, YSD and GBL. All authors approved the final version of the paper.*
Conflicts of interest: *The authors declare that they have no competing interests.*
Financial support: *This work was supported by the National Natural Science Foundation of China, Nos. 81971133 (to GBL), 81671313 (to YSD); the Science and Technology Project of Liaoning Province of China, No. 20180550504 (to PYP); the Medical Science Youth Breeding Project of Chinese People's Liberation Army, No. 17QNP053 (to YSD); the China Postdoctoral Science Foundation, No. 2016M592951 (to YD).*
Institutional review board statement: *All experimental procedures and protocols were approved by the Experimental Animal Ethics Committee of General Hospital of Northern Theater Command (No. 2018002) on January 15, 2018. The experimental procedure followed the United States National Institutes of Health Guide for the Care and Use of Laboratory Animals (NIH Publication No. 85-23, revised 1996).*

Data sharing statement: *Datasets analyzed during the current study are available from the corresponding author on reasonable request.*
Plagiarism check: *Checked twice by iThenticate.*
Peer review: *Externally peer reviewed.*

Open peer reviewer: *Hidenori Suzuki, Mie University Graduate School of Medicine, Japan.*
Additional file: *Open peer review report 1.*

References

Ammirati M, Bagley SW, Bhattacharya SK, Buckbinder L, Carlo AA, Conrad R, Cortes C, Dow RL, Dowling MS, El-Kattan A, Ford K, Guimarães CR, Hepworth D, Jiao W, LaPerle J, Liu S, Londregan A, Loria PM, Mathiowetz AM, Munchhof M, Orr ST, Petersen DN, Price DA, Skoura A, Smith AC, Wang J (2015) Discovery of an in vivo tool to establish proof-of-concept for map4k4-based antidiabetic treatment. Acs Med Chem Lett 6:1128-1133.

Aouadi M, Tesz GJ, Nicoloro SM, Wang M, Chouinard M, Soto E, Ostroff GR, Czech MP (2009) Orally delivered siRNA targeting macrophage Map4k4 suppresses systemic inflammation. Nature 458:1180-1184.

Chen S, Li Q, Wu H, Krafft PR, Wang Z, Zhang JH (2014a) The harmful effects of subarachnoid hemorrhage on extracerebral organs. Biomed Res Int 2014:858496.

Chen S, Feng H, Sherchan P, Klebe D, Zhao G, Sun X, Zhang J, Tang J, Zhang JH (2014b) Controversies and evolving new mechanisms in subarachnoid hemorrhage. Prog Neurobiol 115:64-91.

Chen Y, Zhang Y, Tang J, Liu F, Hu Q, Luo C, Tang J, Feng H, Zhang JH (2015) Norrin protected blood-brain barrier via frizzled-4/beta-catenin pathway after subarachnoid hemorrhage in rats. Stroke 46:529-536.

Collins CS, Hong J, Sapinoso L, Zhou Y, Liu Z, Micklash K, Schultz PG, Hampton GM (2006) A small interfering RNA screen for modulators of tumor cell motility identifies MAP4K4 as a promigratory kinase. Proc Natl Sci U S A 103:3775-3780.

Danai LV, Guilherme A, Guntur KV, Straubhaar J, Nicoloro SM, Czech MP (2013) Map4k4 suppresses Srebp-1 and adipocyte lipogenesis independent of JNK signaling. J Lipid Res 54:2697-2707.

Dong Y, Fan C, Hu W, Jiang S, Ma Z, Yan X, Deng C, Di S, Xin Z, Wu G, Yang Y, Reiter RJ, Liang G (2016) Melatonin attenuated early brain injury induced by subarachnoid hemorrhage via regulating NLRP3 inflammasome and apoptosis signaling. J Pineal Res 60:253-262.

Egashira Y, Zhao H, Hua Y, Keep RF, Xi G (2015) White matter injury after subarachnoid hemorrhage: role of blood-brain barrier disruption and matrix metalloproteinase-9. Stroke 46:2909-2915.

Feiler S, Plesnila N, Thal SC, Zausinger S, Scholler K (2011) Contribution of matrix metalloproteinase-9 to cerebral edema and functional outcome following experimental subarachnoid hemorrhage. Cerebrovasc Dis 32:289-295.

Feng D, Wang B, Wang L, Abraham N, Tao K, Huang L, Shi W, Dong Y, Qu Y (2017) Pre-ischemia melatonin treatment alleviated acute neuronal injury after ischemic stroke by inhibiting endoplasmic reticulum stress-dependent autophagy via PERK and IRE1 signalings. J Pineal Res doi: 10.1111/jpi.12395.

Hao G, Dong Y, Huo R, Wen K, Zhang Y, Liang G (2016) Rutin inhibits neuroinflammation and provides neuroprotection in an experimental rat model of subarachnoid hemorrhage, possibly through suppressing the RAGE-NF-kappaB inflammatory signaling pathway. Neurochem Res 41:1496-1504.

He Y, Xu L, Li B, Guo ZN, Hu Q, Guo Z, Tang J, Chen Y, Zhang Y, Tang J, Zhang JH (2015) Macrophage-Inducible C-Type lectin/spleen tyrosine kinase signaling pathway contributes to neuroinflammation after subarachnoid hemorrhage in rats. Stroke 46:2277-2286.

Ivanidze J, Ferraro RA, Giambrone AE, Segal AZ, Gupta A, Sanelli PC (2018) Blood-brain barrier permeability in aneurysmal subarachnoid hemorrhage: correlation with clinical outcomes. AJR Am J Roentgenol 211:891-895.

Jang M, Cho IH (2016) Sulforaphane ameliorates 3-nitropropionic acid-induced striatal toxicity by activating the Keap1-Nrf2-ARE pathway and inhibiting the MAPKs and NF-kappaB pathways. Mol Neurobiol 53:2619-2635.

Keaney J, Campbell M (2015) The dynamic blood-brain barrier. FEBS J 282:4067-4079.

Lantigua H, Ortega-Gutierrez S, Schmidt JM, Lee K, Badjatia N, Agarwal S, Claassen J, Connolly ES, Mayer SA (2015) Subarachnoid hemorrhage: who dies, and why? Crit Care 19:309.

Li J, Chen J, Mo H, Chen J, Qian C, Yan F, Gu C, Hu Q, Wang L, Chen G (2016) Minocycline protects Against NLRP3 inflammasome-induced inflammation and p53-associated apoptosis in early brain injury after subarachnoid hemorrhage. Mol Neurobiol 53:2668-2678.

Lublinsky S, Major S, Kola V, Horst V, Santos E, Platz J, Sakowitz O, Scheel M, Dohmen C, Graf R, Vatter H, Wolf S, Vajkoczy P, Shelef I, Woitzik J, Martus P, Dreier JP, Friedman A (2019) Early blood-brain barrier dysfunction predicts neurological outcome following aneurysmal subarachnoid hemorrhage. EBioMedicine 43:460-472.

Macdonald RL, Schweizer TA (2017) Spontaneous subarachnoid haemorrhage. Lancet 389:655-666.

Michinaga S, Kimura A, Hatanaka S, Minami S, Asano A, Ikushima Y, Matsui S, Toriyama Y, Fujii M, Koyama Y (2018) Delayed administration of bq788, an etb antagonist, after experimental traumatic brain injury promotes recovery of blood-brain barrier function and a reduction of cerebral edema in mice. J Neurotrauma 35:1481-1494.

Pan P, Zhang X, Li Q, Zhao H, Qu J, Zhang JH, Liu X, Feng H, Chen Y (2017) Cyclosporine A alleviated matrix metalloproteinase 9 associated blood-brain barrier disruption after subarachnoid hemorrhage in mice. Neurosci Lett 649:7-13.

Pan P, Zhao H, Zhang X, Li Q, Qu J, Zuo S, Yang F, Liang G, Zhang JH, Liu X, He H, Feng H, Chen Y (2020) Cyclophilin a signaling induces pericyte-associated blood-brain barrier disruption after subarachnoid hemorrhage. J Neuroinflammation 17:16.

Pannekoek WJ, Linnemann JR, Brouwer PM, Bos JL, Rehmann H (2013) Rap1 and Rap2 antagonistically control endothelial barrier resistance. PLoS One 8:e57903.

Paxinos G, Franklin KBJ (2001) The mouse brain in stereotaxic coordinates, 2nd ed. New York: Academic Press.

Roth Flach RJ, Skoura A, Matevossian A, Danai LV, Zheng W, Cortes C, Bhattacharya SK, Aouadi M, Hagan N, Yawe JC, Vangala P, Menendez LG, Cooper MP, Fitzgibbons TP, Buckbinder L, Czech MP (2015) Endothelial protein kinase MAP4K4 promotes vascular inflammation and atherosclerosis. Nat Commun 6:8995.

Sehba FA, Hou J, Pluta RM, Zhang JH (2012) The importance of early brain injury after subarachnoid hemorrhage. Prog Neurobiol 97:14-37.

Su YC, Han J, Xu S, Cobb M, Skolnik EY (1997) NIK is a new Ste20-related kinase that binds NCK and MEKK1 and activates the SAPK/JNK cascade via a conserved regulatory domain. EMBO J 16:1279-1290.

Sun XG, Duan H, Jing G, Wang G, Hou Y, Zhang M (2019) Inhibition of TREM-1 attenuates early brain injury after subarachnoid hemorrhage via downregulation of p38MAPK/MMP-9 and preservation of ZO-1. Neuroscience 406:369-375.

Tu L, Yang XL, Zhang Q, Wang Q, Tian T, Liu D, Qu X, Tian JY (2018) Bexarotene attenuates early brain injury via inhibiting micoglia activation through PPARgamma after experimental subarachnoid hemorrhage. Neurol Res 40:702-708.

Vitorino P, Yeung S, Crow A, Bakke J, Smyczek T, West K, McNamara E, Eastham-Anderson J, Gould S, Harris SF, Ndubaku C, Ye W (2015) MAP4K4 regulates integrin-FERM binding to control endothelial cell motility. Nature 519:425-430.

Wang M, Amano SU, Flach RJ, Chawla A, Aouadi M, Czech MP (2013) Identification of Map4k4 as a novel suppressor of skeletal muscle differentiation. Mol Cell Biol 33:678-687.

Wu B, Ma Q, Khatibi N, Chen W, Sozen T, Cheng O, Tang J (2010) Ac-YVAD-CMK decreases blood-brain barrier degradation by inhibiting caspase-1 activation of interleukin-1beta in intracerebral hemorrhage mouse model. Transl Stroke Res 1:57-64.

Xu J, Xu Z, Yan A (2017) Prostaglandin E2 EP4 receptor activation attenuates neuroinflammation and early brain injury induced by subarachnoid hemorrhage in rats. Neurochem Res 42:1267-1278.

Xue Y, Wang X, Li Z, Gotoh N, Chapman D, Skolnik EY (2001) Mesodermal patterning defect in mice lacking the Ste20 NCK interacting kinase (NIK). Development 128:1559-1572.

Yang F, Wang Z, Wei X, Han H, Meng X, Zhang Y, Shi W, Li F, Xin T, Pang Q, Yi F (2014) NLRP3 deficiency ameliorates neurovascular damage in experimental ischemic stroke. J Cereb Blood Flow Metab 34:660-667.

Zhang JH, Badaut J, Tang JP, Obenaus A, Hartman R, Pearce WJ (2012) The vascular neural network-a new paradigm in stroke pathophysiology. Nat Rev Neurol 8:711-716.

Zhao H, Pan P, Yang Y, Ge H, Chen W, Qu J, Shi J, Cui G, Liu X, Feng H, Chen Y (2017) Endogenous hydrogen sulphide attenuates NLRP3 inflammasome-mediated neuroinflammation by suppressing the P2X7 receptor after intracerebral haemorrhage in rats. J Neuroinflammation 14:163.

Zhao Z, Nelson AR, Betsholtz C, Zlokovic BV (2015) Establishment and dysfunction of the blood-brain barrier. Cell 163:1064-1078.

Zhu Q, Enkhjargal B, Huang L, Zhang T, Sun C, Xie Z, Wu P, Mo J, Tang J, Xie Z, Zhang JH (2018) Aggf1 attenuates neuroinflammation and BBB disruption via PI3K/Akt/NF-kappaB pathway after subarachnoid hemorrhage in rats. J Neuroinflammation 15:178.

Zuo X, Lu J, Manaenko A, Qi X, Tang J, Mei Q, Xia Y, Hu Q (2019) MicroRNA-132 attenuates cerebral injury by protecting blood-brain-barrier in MCAO mice. Exp Neurol 316:12-19.

P-Reviewer: Suzuki H; C-Editor: Zhao M; S-Editors: Wang J, Li CH; L-Editors: Gardner B, Raye W, Qiu Y, Song LP; T-Editor: Jia Y